BEAM DIAGNOSTICS OF THE 50 MEV PROTON LINEAR ACCELERATOR OF THE ARGONNE ZERO GRADIENT SYNCHROTRON*

M. E. Abdelaziz and R. Perry
Argonne National Laboratory
Argonne, Illinois

Part I - Nondestructive Beam Position Detection

1.1 Introduction

Since the performance and stability of the Zero Gradient Synchrotron (ZGS) are critically dependent on the linac beam behavior, it is found necessary to study the properties of the 50 MeV linac beam for the ultimate purpose of its control by the CDC 924 computer. The first main problem is the beam position, requirements for its detection being: (1) a permanent indication of beam position without beam destruction; (2) a high detection sensitivity with maximum signal-to-noise ratio; (3) a minimum of apparatus complication for possibility of installing position detectors in the limited space available on the beam line.

Some thought was given to electrostatic induction electrodes which are used in some accelerators.[1] One difficulty with this method is that of the electrode dimensions being approximately the same as the particle bunch wave length. A less critical, simpler, and equally reliable method is to utilize magnetic induction in small wire loops due to the 200 MHz component of the beam bunches.[2]

Since the induced loop voltage depends upon several parameters, we have attempted to optimize the design, consistent with our space limitations, by bench tests in which the beam was simulated by means of a conductor carrying a 200 MHz current modulated at the same pulse length as the linac beam.[3] These tests demonstrated that the system has adequately high sensitivity for beam control, which was confirmed by actual beam tests. When the optimized detectors were used to monitor the 50 MeV beam at three locations, they displayed beam position instabilities during the beam pulse. The effect of linac and preaccelerator parameters on beam position have, therefore, been investigated in a series of tests. Variation of several of the parameters caused some degree of beam position displacement. The results indicate the existence of some critical factors which cause beam jitter during machine operation.

*Work performed under the auspices of the U. S. Atomic Energy Commission.

1.2 Calculations of Induced Loop Voltage

Assuming the beam to be filamentary, it is easy to show that, as a first approximation, using simple laws of magnetic induction for an infinitely long beam displaced to a distance 'd' from geometrical center, the voltage difference between a pair of loops which symmetrically monitor the beam is given by[4]

$$V_1 = \frac{\mu_o \omega A}{2\pi} \cdot \frac{I_b}{\frac{a^2 - d^2}{2d}} \quad . \tag{1}$$

If the current-carrying conductor is of finite length 2L, the voltage difference is

$$V_2 = \frac{\mu_o \omega A I_b}{2\pi}\left[\frac{L}{(a-d)\sqrt{(a-d)^2 + L^2}} - \frac{L}{(a+d)\sqrt{(a+d)^2 + L^2}}\right] \tag{2}$$

where

A = loop area, (Fig. 1a)

I_b = peak current

ω = angular frequency .

The propagation velocity is assumed here to be infinite. If, however, a finite velocity of propagation is considered, there will be time delay r/v between current changes and their effect at loop location. This is the case of radiation-retarded fields (RRF) where we could get two field components in the azimuthal and radial directions.[4]

For a finite-length conductor

$$E_\theta = K_1 \left[\int_{-L}^{+L} \frac{e^{-iwt} \cdot e^{+i\frac{w\sqrt{r_o^2+\ell^2}}{v}}}{r_o^2+\ell^2} d\ell - \int_{-L}^{+L} \frac{e^{iwt} \cdot e^{-i\frac{w\sqrt{r_o^2+\ell^2}}{v}}}{r_o^2+\ell^2} d\ell \right]$$

$$+K_2 \left[\int_{-L}^{+L} \frac{e^{iwt} \cdot e^{-i\frac{w\sqrt{r_o^2+\ell^2}}{v}}}{\left(r_o^2+\ell^2\right)^{3/2}} d\ell + \int_{-L}^{+L} \frac{e^{-iwt} \cdot e^{i\frac{w\sqrt{r_o^2+\ell^2}}{v}}}{\left(r_o^2+\ell^2\right)^{3/2}} d\ell \right] \quad (3)$$

$$E_r = -K_3 \left[\int_{-L}^{+L} \frac{e^{iwt} \cdot e^{-i\frac{w\sqrt{r_o^2+\ell^2}}{v}}}{\left(r_o^2+\ell^2\right)^{3/2}} \ell\, d\ell + \int_{-L}^{+L} \frac{e^{-iwt} \cdot e^{i\frac{w\sqrt{r_o^2+\ell^2}}{v}}}{\left(r_o^2+\ell^2\right)^{3/2}} \ell\, d\ell \right] \quad (4)$$

where K_1, K_2, K_3 are constants proportional to current peak and r_o (see Fig. 1b). For an infinitely long wire, integration limits are changed from L to infinity. Calculation results are shown in Fig. 2 for a current at the center for both methods. Linearity with current is also noticed in the experimental results (curve 5). When the conductor is displaced, calculations give deflection curves in Fig. 3. Sensitivity to transverse displacement of current, in bench tests, is shown in Fig. 4. Voltage variation with distance is the same, except that values are higher in the RRF method. In the optimized system, the experimental value of about 5 mV/mm/mA agrees more reasonably with RRF values, as will be seen later. The difference between loop voltage difference for an infinitely long and a finite length conductor is relatively small.

1.3 Experimental Characteristics of Loop Position Detectors

The experimental setup for simulating the beam is shown in Fig. 5, where a copper conductor carries a 200 MHz current modulated with the same pulse as that of the beam. The demodulated loop voltage is fed into a 50 Ω line via amplifiers utilizing 709 operational IC amplifiers with appropriate feedback, frequency compensation, and emitter follower termination. The loop container is carefully shielded, and transistor diodes are strictly identical. Matching between the loops and the rf detectors is provided with coaxial stubs. Some of the factors that affect resonance conditions of the loop are: loop size, geometry, and number of turns as well as conductor diameter. Samples of bench results are shown in Figs. 6 and 7.

In general, the loop voltage follows theoretical expectations, the difference being due to the loop and coupled impedances which were not considered in theoretical calculations.

In the final optimized system, loops as shown in Fig. 7 (No. 1) were used in monitoring the 50 MeV beam at three locations: BPD 502, BPD 503, and BPD 601 (Fig. 8). Over a considerable length of time during machine operation, beam position instabilities were noticed from pulse to pulse and sometimes during the same pulse (1). Fig. 9 shows a sample of what happens to beam position when some linac parameters are changed for one reason or other; in this case machine tuning necessitated rf gradient adjustment. Traces are taken on a storage scope which indicate also constancy of beam current.

Calibration curves of beam position detectors are obtained by steering the beam with SM 501 and SM 502 (Fig. 8) in horizontal and vertical planes. For each position beam profiles are taken using a narrow slit and X-Y plotter. A sample of these calibration curves is shown in Fig. 10 indicating a loop detection sensitivity of 5 mV/mm/mA.

1.4 Effect of Linac Parameters on Beam Position

In these tests, position detectors BPD 502 and 503 were the optimized high sensitivity detectors, while 601 was not. However, results for the three detectors are included for comparison.

1.4.1 Effect of Ion Source Parameters.

Varying the ion source parameters, while maintaining the beam current constant, position displacement occurred in the manner shown in Fig. 11 for vertical deflection. Horizontal deflection took

place at a smaller rate. The change of the duoplasmatron constants would naturally cause deformation of the source's plasma boundary such that ion trajectories are consequently deflected.

1.4.2 Effect of RF Gradient in the Tank. Because of its effect on beam jitter, this effect was investigated in three separate runs. The first at a beam current of 20 mA, the gradient being detected with the tank loop No. 23. Results are shown in Fig. 12 (vertical and horizontal respectively); such variations are confirmed by beam profiles using a slit and X-Y plotter. The same results were obtained in the second run with smaller magnitudes.

The substantial change in beam position is not clearly understood. However, the question could be raised whether the existence of rf modes in the tank other than the 010 mode could have an effect on the resultant rf field in the tank. The presence of modulation in rf amplitude at frequencies of 34.8 kc and 104 kc in our linac was established.[5] Existence of such frequencies was interpreted in terms of beats between the TM 010, TM 011, and TM 012 modes.[6] There was also the question of betatron oscillation in the linac tank and their effect on position instabilities when the beam is initially off center. To test the validity of this statement, a third run was carried out after steering the beam in the preinjector region to machine center. Results shown in Fig. 13 indicate that position changes with rf gradient are still high.

1.4.3 Effect of Linac Drift Tube Quadrupole Current. Changing the current in the last group of linac quadrupoles showed another substantial position displacement. In the 15 mA run, we made the current change in the first series of drift tubes and found position displacement at a rate that reached .2 mm per 1% (Fig. 14).

Position changes occurred also with current change in the 50 MeV quads (QM 503 and 504) as shown in Fig. 15.

In all this the transverse beam displacement effect is due to beam assymetry with respect to focusing elements. This may be either simple lens misalignments, nonuiform density within a symmetrical beam, or a uniform beam whose center of gravity is displaced such that change in some focusing element, including the rf accelerating field strength, causes a lateral shift of the beam.

1.5 Conclusions

Reasonable agreement has been found between calculated and measured voltage differences induced by 200 MHz current in two carefully designed rf loops as a function of displacement of the current from the midpoint between the loops. Careful measurements with a 50 MeV linac beam confirm that beam position detection is in agreement with bench tests, and that the sensitivity (5 mV/mm/mA) and the position resolution (±0.1 mm) are adequate for use with automatic control of parameters which affect beam position. Several linac parameters have been found to effect beam position changes. The most significant one for automatic control has not yet been established; but it is anticipated that some one parameter will be connected to the control computer, using the beam position detector as the sensing element, in order to maintain optimum beam position for the ZGS.

Part II - A Method for Rapid Measurement of Beam Emittance

2.1 Introduction

Extensive work in different laboratories has been carried out for the measurement of transverse phase space properties of accelerated beams. This is usually done in order to attain a better understanding of emittance-acceptance matching problems. Attempts have always been aimed at improving measurement techniques for higher accuracy and, more important, faster beam scanning for the observance of emittance variation with time from pulse to pulse and within the pulse. It is possible by nondestructive means to obtain beam profiles at three locations along a beam, from which an approximate knowledge of the beam emittance can be deduced;[7] but for detailed knowledge of the phase-space density, a destructive method appears to be required.

The common technique of two slits (or pairs of slits) is relatively slow. The four-dimensional phase volume is obtained using crossed slits and photographic films.[8] A more refined technique uses a growing magnetic field to determine angle limits of beam samples from an upstream slit. The emittance pattern using this method could be displayed on the scope in one minute over a number of pulses.[1,9] Emulsion technique is also applied in phase space measurements.[10,11]

A more advanced method for partial or total emittance measurement within the pulse time was achieved by using sampler and analyser magnets (kickers) thereby eliminating the use of slits.[12] In another approach, alternating electric fields were used to scan beam samples across a downstream slit.[13]

It is seen from these methods that in order to obtain total emittance over one pulse, the

equipment must be complicated and extremely costly. Otherwise, one must obtain average emittance values over a number of pulses as is done by a growing magnetic field. Our method, however, has the same advantage of fast emittance measurement over a number of pulses but with the feature of simplicity and economy. In addition, density distribution in transverse phase space can be obtained in detail and as a function of time during the beam pulse.

2.2 Description of the Method

The system consists of a multi-channel strip collector which, together with an upstream narrow slit, scans the beam transversely in less than a minute. At each position (corresponding to a pulse) current signals from the multi-channel collector are fed to a multiplexer via separate amplifiers (Fig. 16). In the multiplexer (described elsewhere, ref. 2) electronic switching from one channel to the other takes place at 1 μsec intervals. Thus, in 10 μsecs, corresponding to 10 channels, a density distribution in phase is displayed on a scope and is recorded in a computer. Then the multiplexer switches over to the first channel again and another scan of the same channels is obtained giving another density distribution. This procedure is repeated many times during the pulse. Thus the density distribution pattern indicates all variations during the pulse. In preliminary tests, 10 strips were used each of which was .060" wide, .350" thick and separated by a gap of .020". The strip collector was installed in BR 601 box 100 in downstream from a .020" slit in BR 502 box (Fig. 8). The angular resolution in this setup is .8 milliradian. A sample of the scope density distribution patterns showing density variation during the pulse is given in Fig. 17. From the detailed computer data, which are confirmed with scope traces, the emittance figures were computed to give a series of ellipses (Fig. 18) containing 80% of total beam current. Although each ellipse represents emittance area over a number of pulses (16 in this case) yet the change of angular limits during the pulse is obvious from successive figures at 10 μsec intervals.

Since the detected signal level was adequately high, a further improvement of resolution was possible through reducing strip width from .060" to .021" and the gap from .020" to .014", the resulting angular resolution was thus reduced to 0.35 milliradian. Using this device, the number of channels displayed on the phase-density pattern was more than doubled. Samples of such patterns are shown in Fig. 19 for the refined scheme. The linac emittance using this technique was measured under different linac conditions. More details are being prepared for later publication in an internal report.

2.2.1 Effect of δ-Ray Emission. Since the accuracy of emittance measurements in our device depends on accuracy of ion collection by strips the question of δ-ray and secondary electron emission arises. The latter is a surface effect which will be proportional to density of primaries such that it will not change the shape of the distribution pattern. Otherwise, it will proportionally improve the level of detected signals.

On the other hand, the more penetrating δ-rays will be mainly emitted from strip sides, as the height of strips is greater than that required to stop 50 MeV protons. A δ-ray detector equipped with two copper strips identical to those in the emittance device and a δ-ray measuring plate (Fig. 20) was installed in the BR 601 box to receive the proton beam from a .020" slit in the BR 502 box. Over many runs it was noticed that the δ-ray signal is extremely small compared with the main strip proton signal, less than .1% as illustrated by scope traces of Fig. 21. Thus the effect of both secondary electrons and δ-ray is negligible.

2.3 Conclusion

The beam emittance of a 50 MeV beam has been measured in less than one minute, using a slit and multi-strip collector with an angular resolution of 0.35 milliradian for beam scanning. A multiplexer was used to sample the 10-channel collector every 10 μsecs. Data displayed on an oscilloscope and recorded in a CDC 924 computer gives the density distribution in phase space at 10 μsec intervals during the beam pulse.

Acknowledgement

It is difficult to mention all personnel who assisted in this work. However, the continuing interest of R. Martin is acknowledged. We wish also to thank R. George for performing computer work in beam position calculations. Thanks are also due W. DeLuca for furnishing the multiplexer facility, and the computer group for carrying out computer work for beam emittance. Appreciation is also expressed to all the technical personnel who contributed in different aspects of the project.

References

1. R. Allison and et al, Proceedings of the 1966 Linear Accelerator Conference, October 1966, LA-3609.
2. Private Communication from N. West, R. H. E. L.
3. M. E. Abdelaziz, Internal Report MEA-5, Accelerator Division, Argonne National Laboratory, September 20, 1967.

4. M. E. Abdelaziz, Internal Report, MEA-6, Accelerator Division, Argonne National Laboratory, (Under Publication).

5. L. Lewis and et al, Sixth International Conference on High Energy Accelerators, Cambridge, Mass., September 1967.

6. T. Nishikawa, AADD-87, Brookhaven National Laboratory, Accelerator Department, November 15, 1965.

7. W. H. DeLuca, M. F. Shea, Linear Accelerator Conference, Brookhaven National Laboratory, May 1968.

8. I. F. Ivanov and et al, Method is described by A. van Steenbergen, Nuclear Instruments and Methods, 51 (1967), p. 248.

9. B. Vosicki, Proceedings of the 1966 Linear Accelerator Conference, LA-3609.

10. T. J. Sluyters, Nuclear Instruments and Methods, 27, 301 (1964).

11. C. Bovet, M. Regler, CERN/MPS/LIN 64-2.

12. T. J. Sluyters, R. Damn, A. Otis, BNL 11111.

13. Batalin and Moguchev, Translated from Pribory i Technika E'ksperimenta, No. 5, pp. 26-32, September-October 1966.

DISCUSSION

(R. Perry)

ALLISON, LRL: We see the same beam position shifts as experienced at Argonne and reported on them at the last conference. Since then we have tried to find out the cause. We checked drift tube alignment, etc. We discovered that a misalignment in the preinjector increased the "position sweep" by a factor of 10 over that normally seen. At 40 feet from the exit of the linac the fast position jitter got as high as 1/2 inch. By means of scintillators we discovered that the position sweep was accompanied by a change of emittance or focus. These are disturbing effects if the beam is to be injected into a synchrotron and we have not found the cause yet.

PERRY, ANL: We get much "static" from the synchrotron people but it is not clear how these factors affect them since they also have many factors.

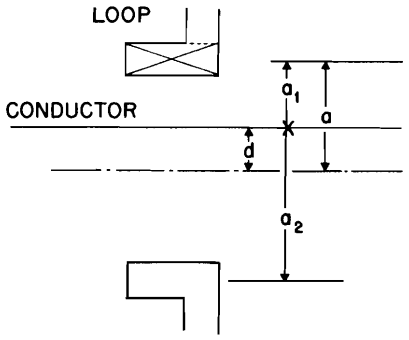

Fig. 1a Loop and Conductor

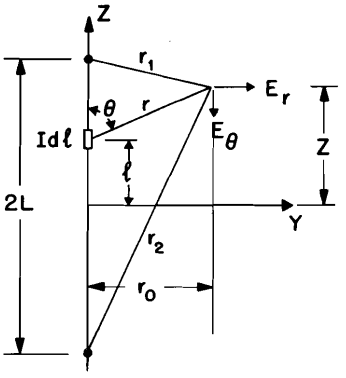

Fig. 1b Loop and Conductor

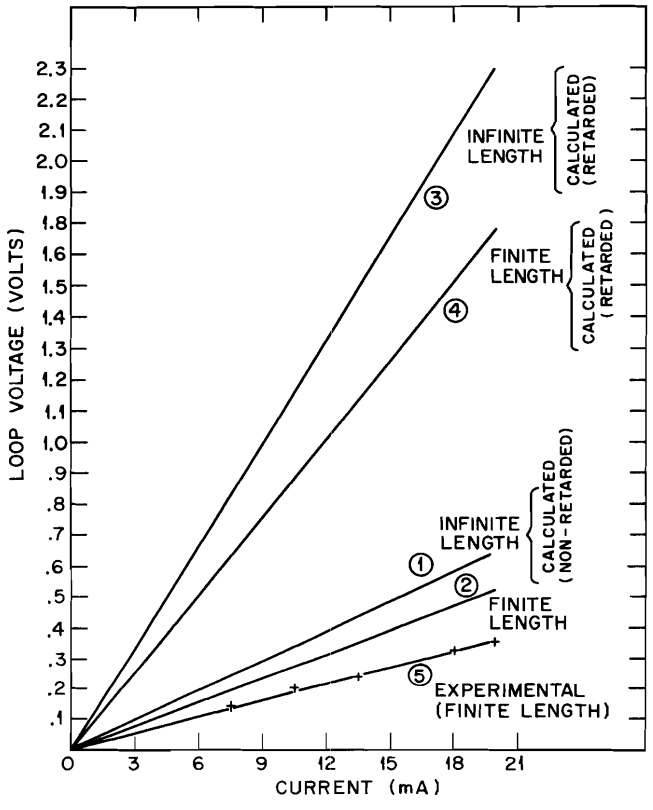

Fig. 2 Calculated and Experimental Values of Loop Voltages (Central Conductor)

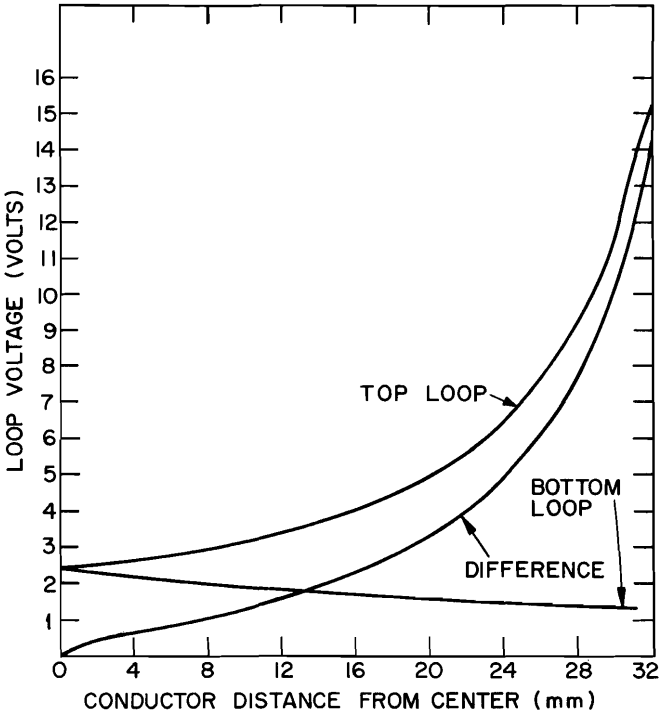

Fig. 3 Calculated Loop voltage using Radiation-Retarded-Field Method (Infinitely Long Conductor, I = 20 mA)

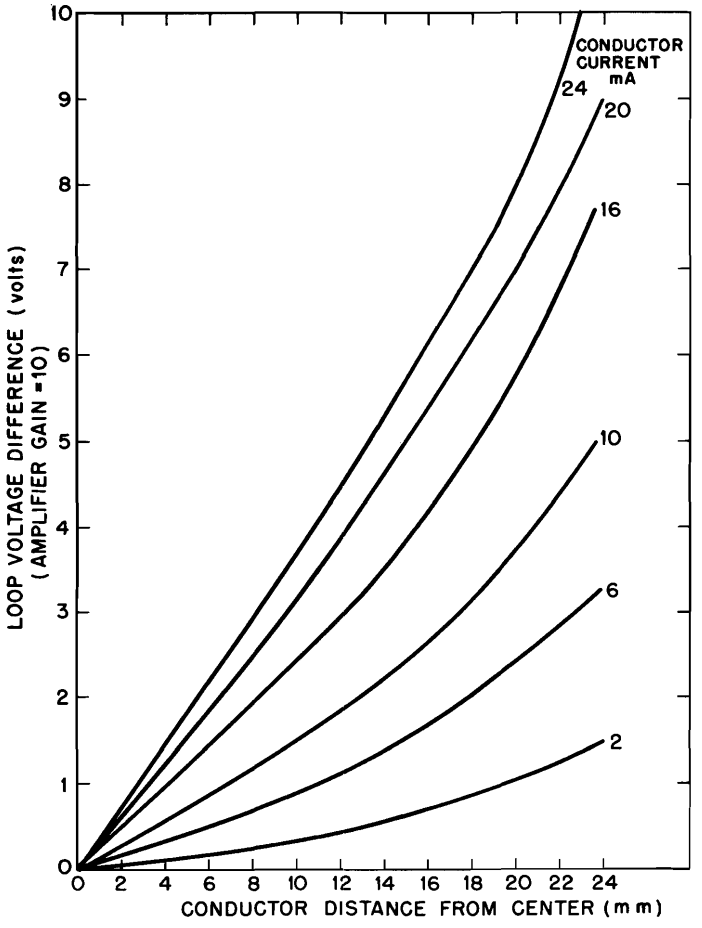

Fig. 4 Differential Sensitivity to Transverse Displacement of Current, for Large Loops

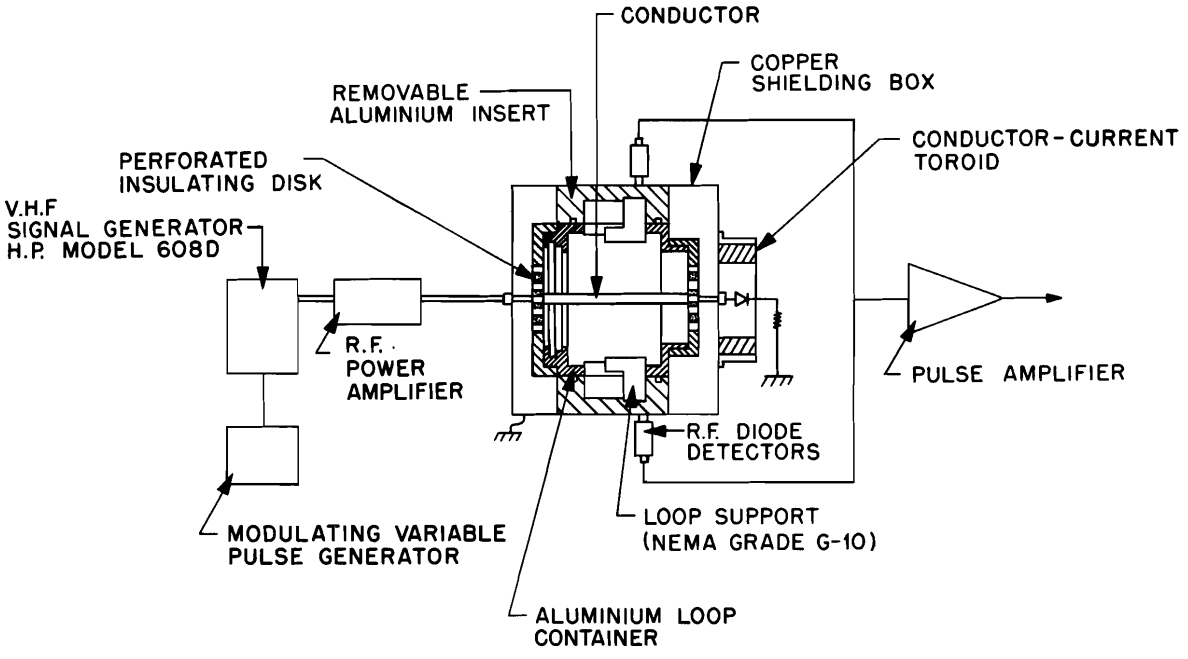

Fig. 5 Experimental Set-Up for Bench Tests of Loop Detectors

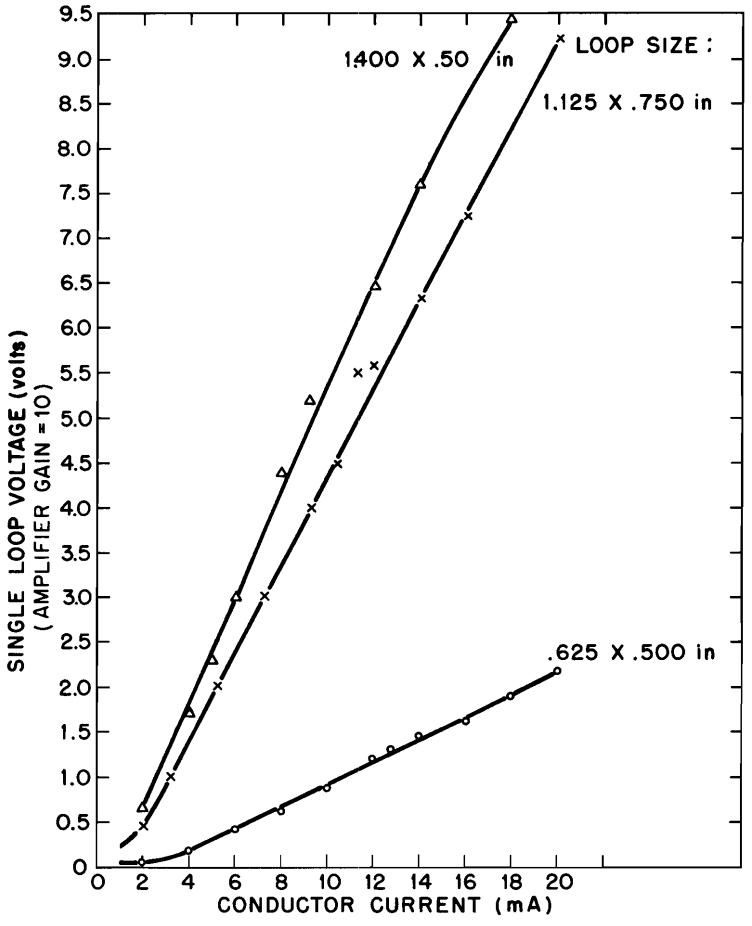

Fig. 6 Effect of Loop Size (Central Conductor)

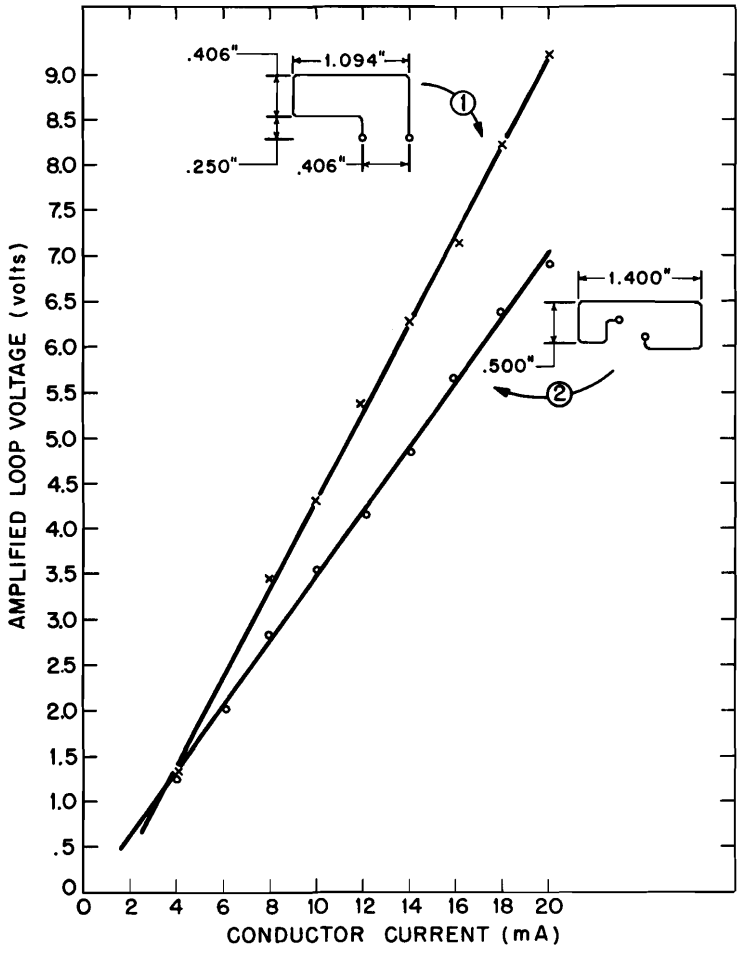

Fig. 7 Effect of Coil Geometry on Detection Characteristics

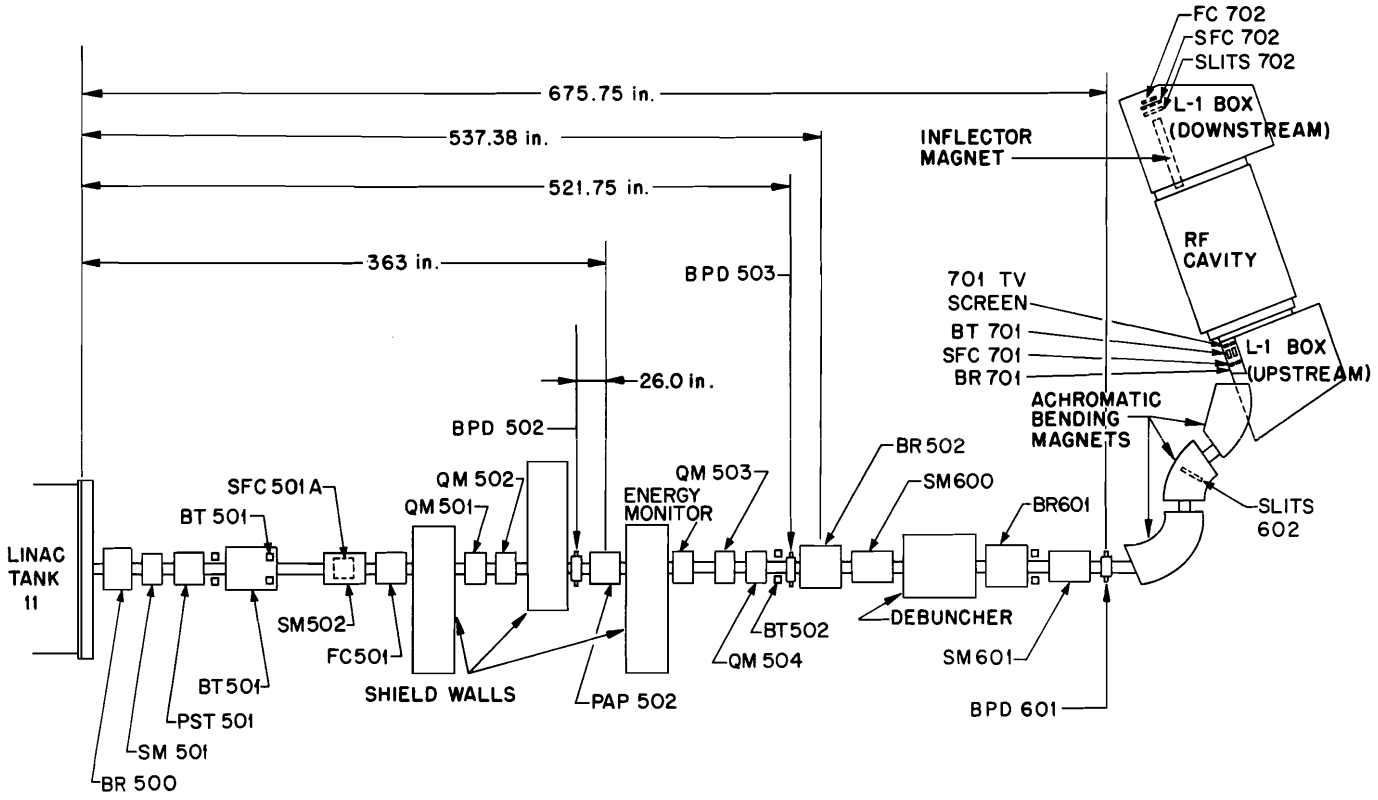

Fig. 8 Location of Linac Components, 500 and 600 Areas

a. Starting Point - Top Trace- Beam position signal from BPD 502 V (1 V/ scope div.)

Bottom Trace - Beam Current signal from BT 701, 10 mA/ scope div.

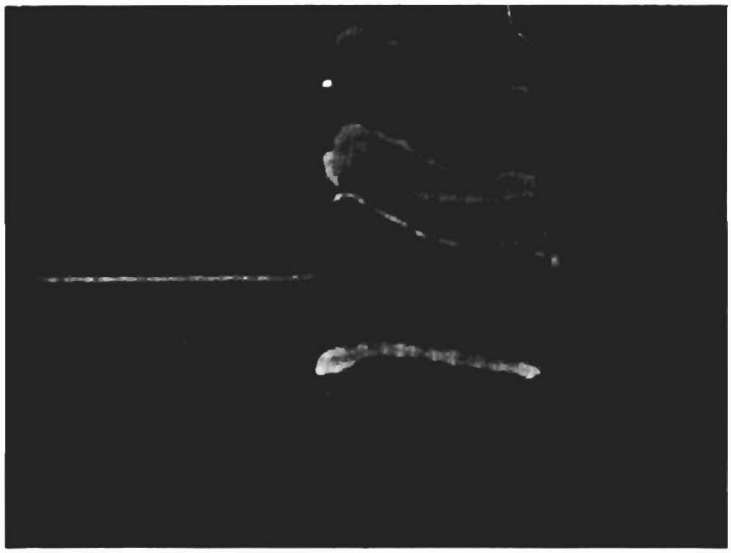

b. One Hour Later
BPD 502 V, (1 V/ scope div.)

BT 701, 10 mA/ scope div.

Fig. 9 Sample of Beam Position Instabilities During Machine Operation, Beam Current Being Constant

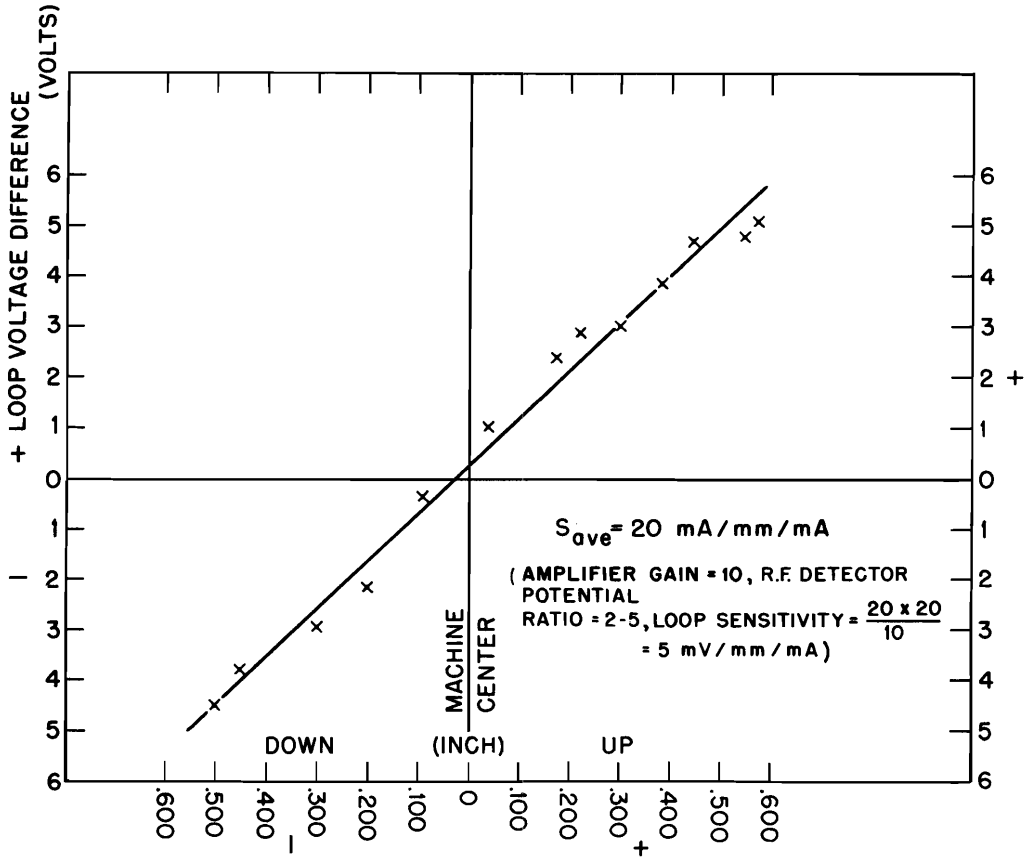

Fig. 10 Calibration Curve of BPD 503 (Vertical Deflection)

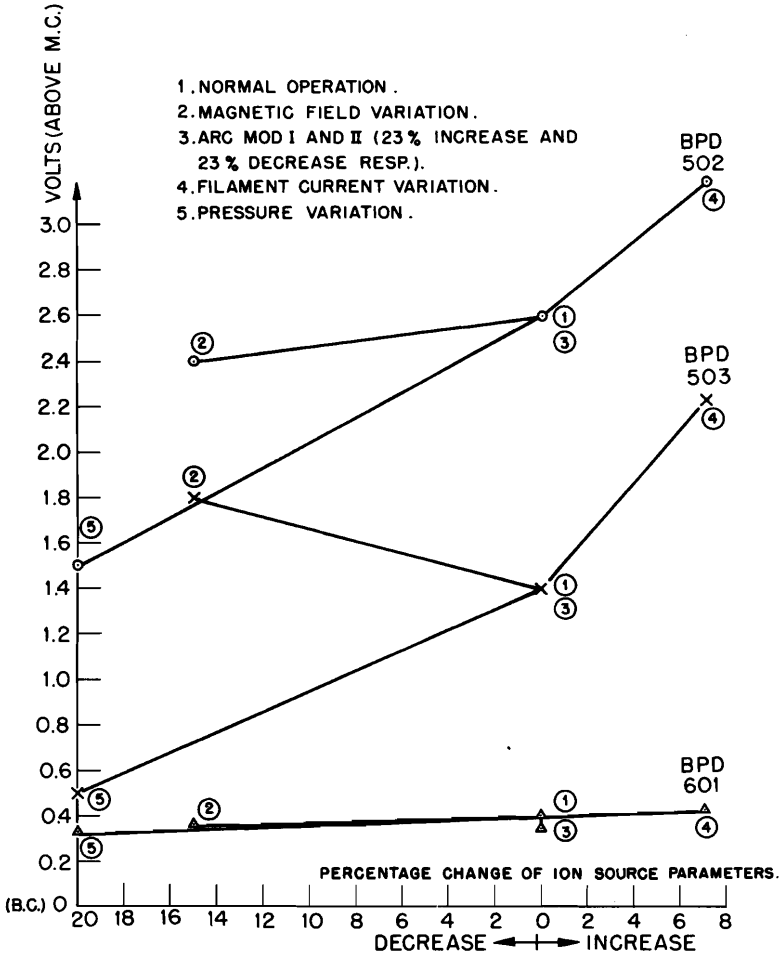

Fig. 11 Effect of Ion Source Parameters on Beam Deflection in Vertical Plane

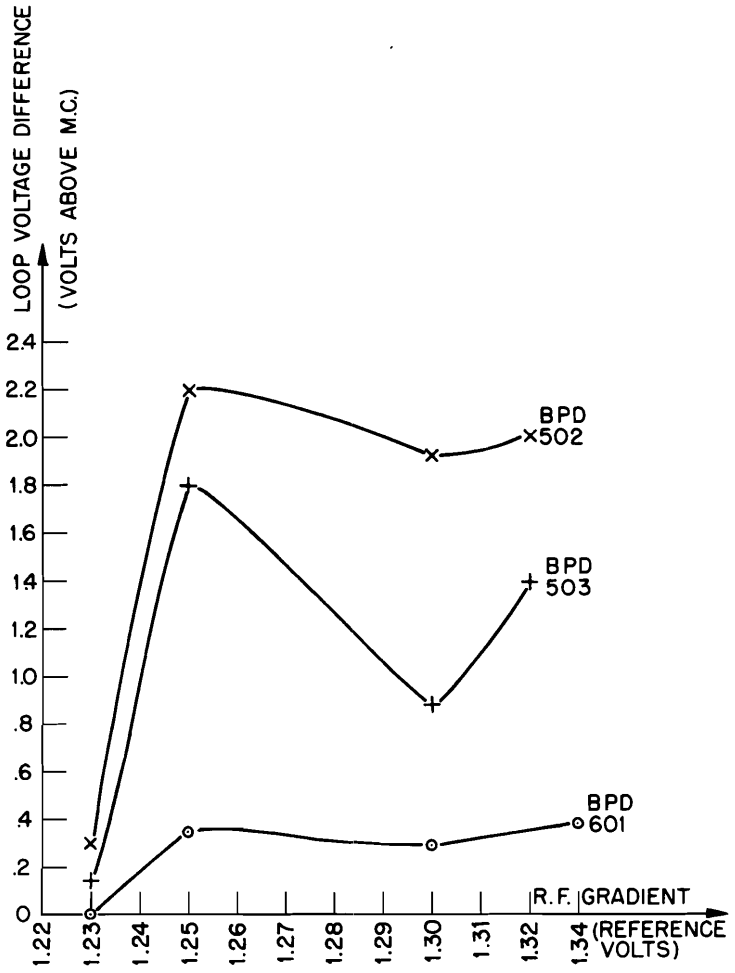

Fig. 12 Effect of R. F. Gradient Level on Vertical Deflection (Loop 23)

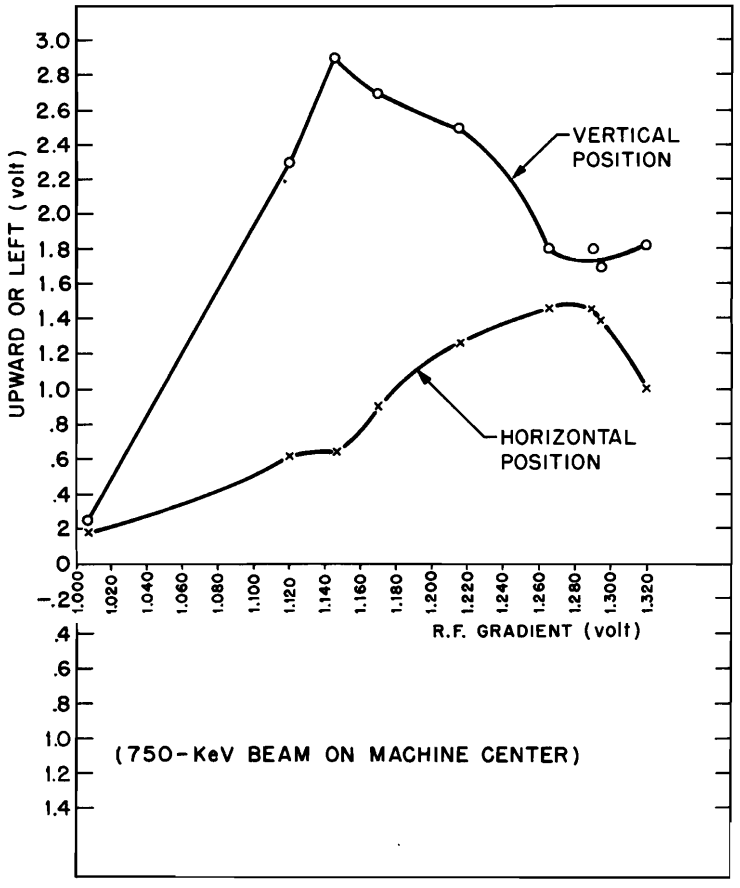

Fig. 13 Effect of R.F. Gradient Variation on Beam Position at BPD 502

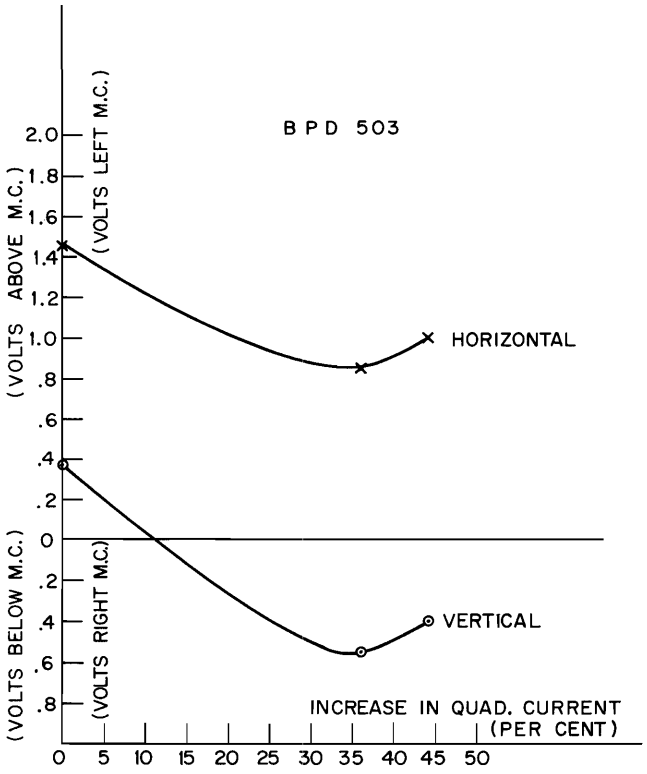

Fig. 14 Effect of increasing Drift Tube Quadrupole Current (Rect. 1) on Vertical and Horizontal Beam Deflections.

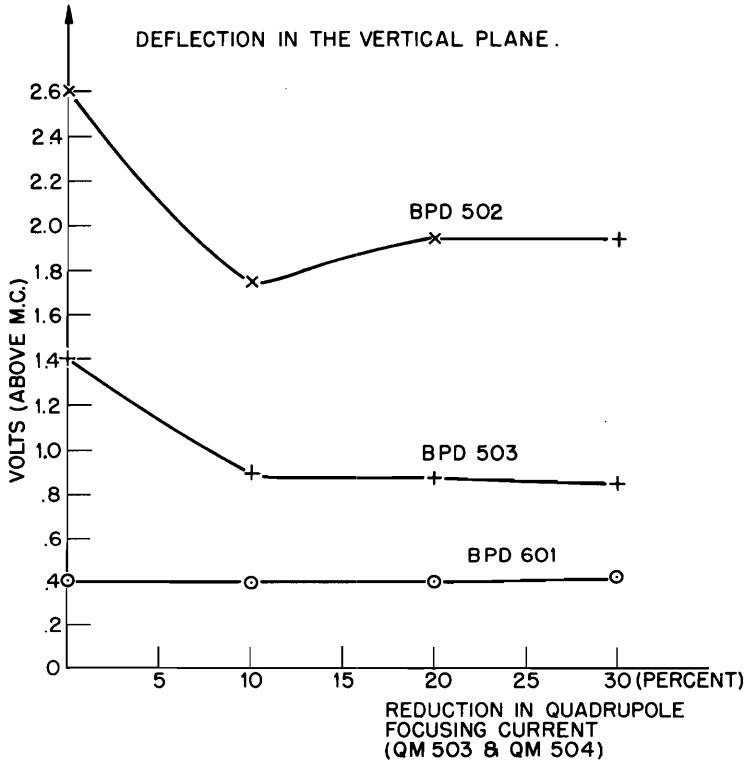

Fig. 15 Effect on Reducing Quadrupole Focusing Current in QM 503 and QM 504 on Beam

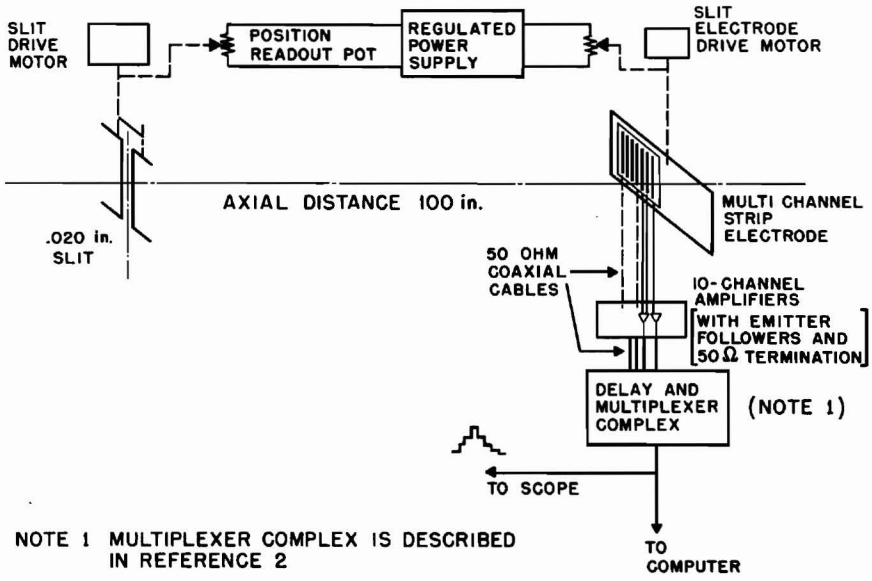

Fig. 16 Schematic of Phase Space Density Measurement

Collector center 0.3 in. from beam axis

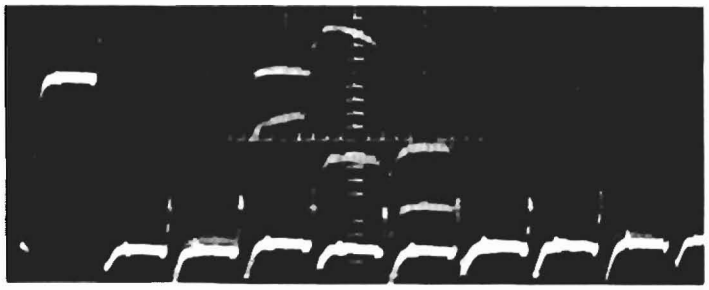

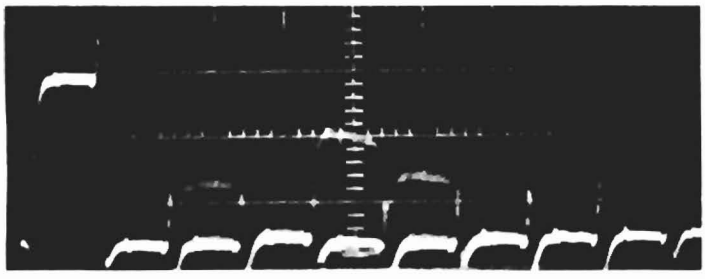

Collector center 0.6 in. from beam axis

Fig. 17 Phase-Density Distribution Patterns from Multi-Strip Collector

(Resolution = 0.8 mrad) 0.2 V/cm, 1 μsec/cm

(NOTE: Signal on left channel externally applied for identification)

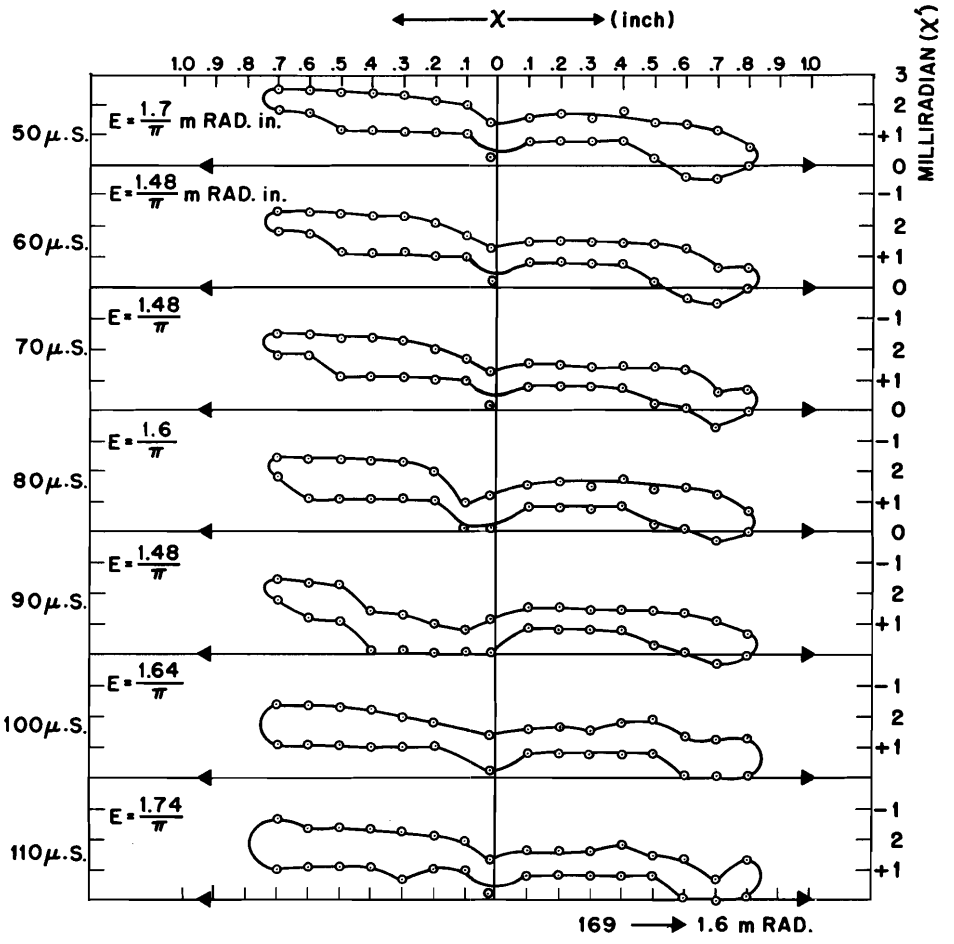

Fig. 18 Emittance Figures Enclosing 80% of Total Beam Current in the 50 MeV line.

(Resolution = .35 mrad)

Eight Strips (.2 V/cm)

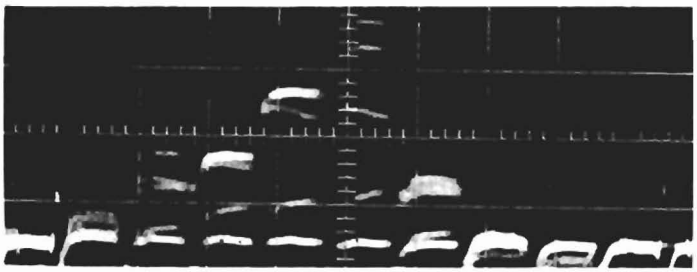

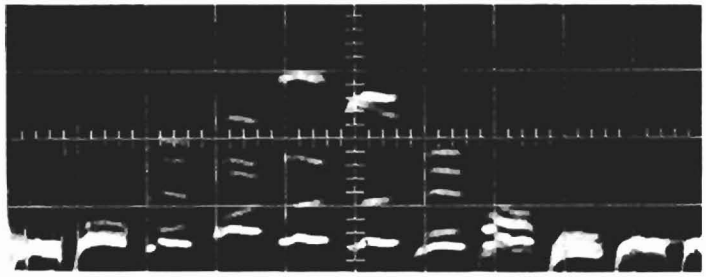

Nine Strips (.1 V/cm)

Fig. 19 Phase-Density Distribution Patterns Taken With Multi-Strip Collector

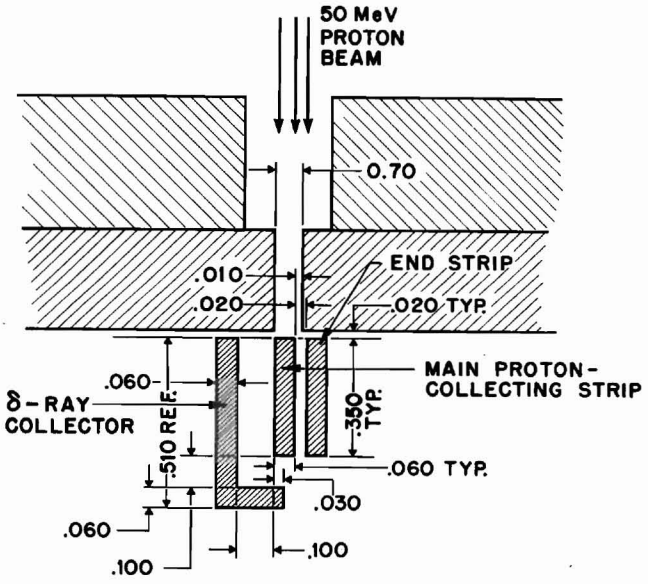

Fig. 20 δ-Ray Detector

(NOTE: All amplifiers are phase reversing.)

Top - Background base (no beam) for δ-ray .01 V/div., 50 μsec/ div.

Bottom - RF tank gradient

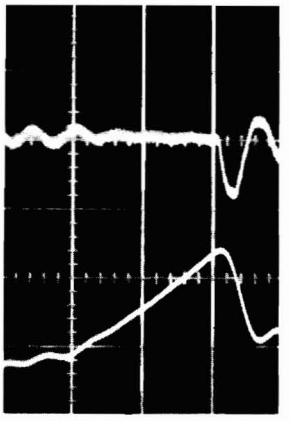

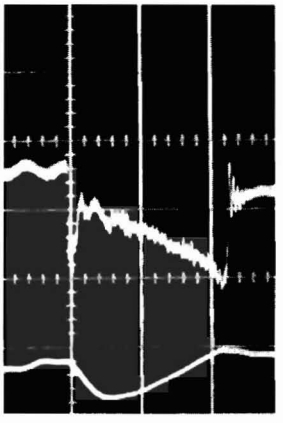

Top - Signal from δ-ray collector with beam. .01 V/div. (amplifier gain = 100)

Bottom - RF tank gradient

Top - Signal from end collector strip, .005 V/cm, (amplifier gain = 10)

Bottom - Signal from main strip, 1 V/cm, (amplifier gain = 10)

Fig. 21 δ-Ray Signal Compared With Main Strip Signal